Polarimetric Decomposition Analysis of Lunar North Pole Crater Hermite-A Using Chandrayaan-2 DFSAR Data

Mulkala Saritha[1]
ECE Department
National Institute of Technology,
Warangal, India-506004
ms23ecr1r13@student.nitw.ac.in

Dr. Kiran Dasari[2*]
(Corresponding Author)
Department of Mechatronics Engineering
Manipal Institute of Technology,
Manipal Academy of Higher Education,
Manipal, Karnataka, India-576104
kiran.dasari@manipal.edu

Lokam Anjaneyulu[3]
ECE Department
National Institute of Technology,
Warangal, India-506004
anjan@nitw.ac.in

***Abstract*—Chandrayaan-2 launched in the year of July 22, 2019 consisting of different types of sensors to map the lunar surface. It integrates Synthetic Aperture Radar (SAR) at two wavelengths (L and S band) at various resolutions with numerous polarimetric ways in a lightweight configuration (about 20 kg). The computation of the 2x2 complex scattering matrix for each resolution cell can be obtained from the DFSAR (Dual Frequency Synthetic Aperture Radar) which enables the characterization of the lunar surface at different incident angles, wavelengths in terms of polarization properties of the radar. This paper mainly focuses on various decomposition techniques and analysis of backscattering coefficients of the lunar surface using full polarimetric L-band DFSAR data. The data is collected from PSR (Permanent Shadowed Region) of lunar north polar Hermita Crater.**

***Index Terms*—Chandrayaan-2, Hermite-A,RADAR, Polarimetric Decomposition, SAR, Moon, DFSAR, Lunar North Pole, PolSAR Pro.**

I. Introduction

The physical properties of the lunar surface is complicated to understand the geomorphological history and analysis of their potential exploration. The near-surface physical features of the regolith are essential for recognizing the spatial boundaries and comparative timeline of mare flow elements and impact-related activities,which ultimately affect the spatial variations in surface and subsurface composition. Dielectric properties and structural information of the lunar surface can be provided PolSAR data in the form of backscattered values, these values are represented in scattering matrix. MIDAS(Microwave Data Analysis Software) is one optimal tool provided by ISRO (Indian Space Research Organisation) for the analysis of impact craters, roughness of the surface ejecta deposits and associated impact melt. Back scattering of the radar waves is useful to know the structure of the subsurface as well. Implementing new radar observations across multiple wavelengths can help to better define the sizes of surface blocks and differentiate between surface and subsurface rocks in both nearby and far ejecta deposits DFSAR onboard India's Chandrayaan-2, is the second lunar machine operated outside Earth's Orbit and it is represents the first FP SAR (Synthetic Aperture Radar). This DFSAR system supports polarimetric operational modes and supports the planetary and lunar surface applications. Regarding lunar surface applications the biggest improvement gives with this device are as follows: In earlier the moon data obtained from the orbital radars like Mini-SAR and Mini-RF as well as from ground based systems. Mini –RF and Mini-SAR operated at P,S,X frequency bands, wavelengths are 70cm , 12.6cm and 3.8cm respectively, the penetration depth of dry ,low-loss soil around 3meters at L-band SAR. It demonstrates a notable sensitivity to ilmenite concentration and is capable of detecting surface or subsurface rocks with diameters approximately one-tenth of the radar wavelength (around 2 cm) or greater. [1]. In addition, when utilized alongside the S-band radar (12 cm wavelength) and the data collected from the Mini-SAR on Chandrayaan-1 as well as the Mini-RF on the Lunar Reconnaissance Orbiter (LRO), the DFSAR demonstrates the capability to effectively illustrate the radar scattering properties of the uppermost patterns of the lunar surface.

The DFSAR is designed for polarimetric imaging radars in planetary missions with a fully polarized (FP) configuration, where each pixel in the image data is represented in the form of 4 × 4 scattering matrix. In FP device transmits and receives the signal in to two orthogonal polarization (HH, HV, VH, and VV), from this single or dual polarization properties gives the enhanced information extraction from the image. In this context, "H" denotes Horizontal, and "V" denotes Vertical. The following terms are defined: "HH" refers to horizontal transmission and horizontal reception, "HV" indicates horizontal transmission and vertical reception, "VV" signifies vertical transmission and vertical reception, and "VH" represents vertical transmission and horizontal reception. In this notation, the first letter signifies the transmission mode, while the second letter indicates the reception mode [2].

979-8-3315-3469-1/24/$31.00 ©2024 IEEE
DOI 10.1109/ICPIDS65698.2024.00078

A. Overview of the DFSAR Instrument

DFSAR is a specialized instrument for capturing high-resolution radar data of planetary bodies, especially the Moon, to study surface composition, texture, and structure. It operates in two Frequency bands—S-band and L-band and it operates in quad-polarization and compact polarization (efficient data collection) modes for analyzing surface scattering properties. Additionally, it captures data from multiple viewing angles to create accurate models of surface features. DFSAR onboard Chandrayaan-2 it provides high resolution images of lunar surface at two frequency bands L and S band. The two radar systems share a common microstrip planar antenna, allowing for both standalone and synchronous L/S-band imaging. DFSAR utilizes chirp signals (LFM-Linear Frequency Modulated commonly referred as chirp) with selectable bandwidths (75 MHz to 2 MHz), providing flexibility in surface and subsurface imaging [3]. The system incorporates distinct transmit chains for horizontal (H) and vertical (V) polarizations, utilizing high-efficiency gallium-nitride-based solid-state power amplifiers (SSPAs) to ensure power-efficient transmission. The SSPAs contains phase shifters for quad or full polarization enabling precise control over radar signals. DFSAR system more compatible in the on board range compression that reduces data volume by 70%, it also provides high signal to noise ratio ensured by low-noise, high-gain amplifiers. FP mode captures detailed Polari metric data (HH, HV, VH, and VV) for analyzing lunar surface characteristics, while hybrid/compact polarization mode offers a more efficient option. Top level specifications of DFSAR system for L-Band and S-Band [4]: Altitude: 100km, range swath: 10km, incidence angle: $9.6°-36.9°$, resolution: 2-75 m, chirp width: 75-2MHz, receiver gain: 90dB, Data rate: 190Mbps, raw bus power: 100W, Payload mass: 20kg, cross polarization : $> 30dB$ and maximum duty cycle: 24%.

II. SENSOR CONFIGURATION AND DATASETS USED

The DFSAR onboard Chandrayaan-2 operates at L-band (1.25 GHz) and S-band (2.5 GHz) frequencies, capturing data in both Full polarization and compact-polarity modes. This allows the radar to provide detailed insights into the lunar surface and subsurface properties through multiple look and various incidence angles. In this study, L- band frequency datasets were collected near the Moon's North Pole in fully Polari metric mode 30°, respectively. The calibrated DFSAR Seleno-referenced images (SRI) dataset, processed and analyzed using the MIDAS. For the fully polarimetric dataset, the Scattering Matrix [S] and Coherency Matrix [T3] were derived, while the compact polarimetric dataset produced the Covariance Matrix [C2]. To improve image quality and to reduce speckle noise, multilook and a Refined Lee filter with a 5 x 5 window size was applied, generating images with a resolution of 20 meters x 20 meters. The processed datasets offer significant insights into the composition and scattering characteristics of the lunar surface, thereby enhancing our understanding of the Moon's geology.

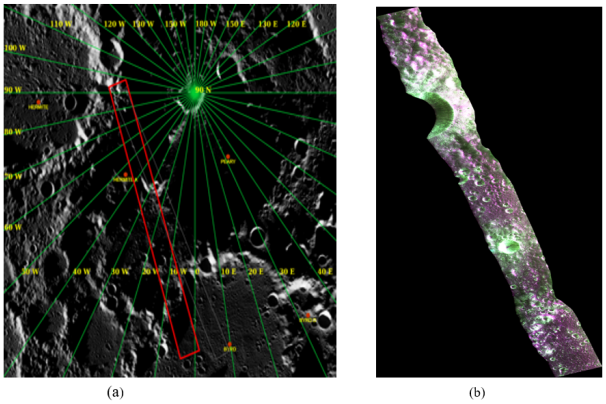

(a) (b)

Fig. 1. (a) Data acquisition by the Chandrayaan-2 Dual Frequency Synthetic Aperture Radar (DFSAR) over the North Pole region. (b) Hermit-A Region

A. Software Functionalities

MIDAS provides an intuitive interface along with a variety of sophisticated features that enhance the processing and examination of DFSAR data. Its capability to manage both full- and hybrid-polarimetric data makes it an essential resource for lunar studies, allowing for in-depth analysis of lunar surface and subsurface characteristics. In addition it supports the analysis of space borne and airborne sensors data, it also supports the polarimetric and radiometric calibration of Chandrayyan-2 DFSAR data. Chandrayaan-2 SAR data has been downloaded from "www.issdc.gov.in" website at North polar Hermit-A region. StudyArea: ch2_sar_ncxl_20191017t234531221_d_fp_d18 As shown Fig.1(a) is a North Polar Region of the Lunar surface in this image the highlighted red color strip represents the Hermite-A Region. Fig.1(b) represents the acquisition of DFSAR data from the Chandrayaan-2 mission over the specific Hermite-A region.

III. METHODOLOGY

To study the characterization of lunar surface using DFSAR Dataset, calibrated data of DFSAR at particular region of the lunar surface downloaded from ISSDC (Indian Space Science Data Centre) website. In this paper we focused on the various decomposition and classification at North Pole Hermit-A region as shown in Fig.1, the product ID of Study Area: ch2_sar_ncxl_20191017t234531221_d_fp_d18; ch2- represents the Chandrayaan-2 , sar- represents the Synthetic Aperture Radar, ncxl-L band data, yearmmdd, fp-full polarization and d18- is orbit number. The Fig.2 explained about the detailed procedure to achieve the polarimetric parameters of Hermit-A region using Yamaguchi and H-A-alpha Decomposition techniques [5]. This analysis done using MIDAS for generation of covariance matrix, Multilooking, Filtering and Decomposition [6]. DFSAR Data will be The information is utilized to analyze characterization and physical properties of moon surface, crater types, their impact, regolith layer and presence of minerals. DFSAR data is sufficient

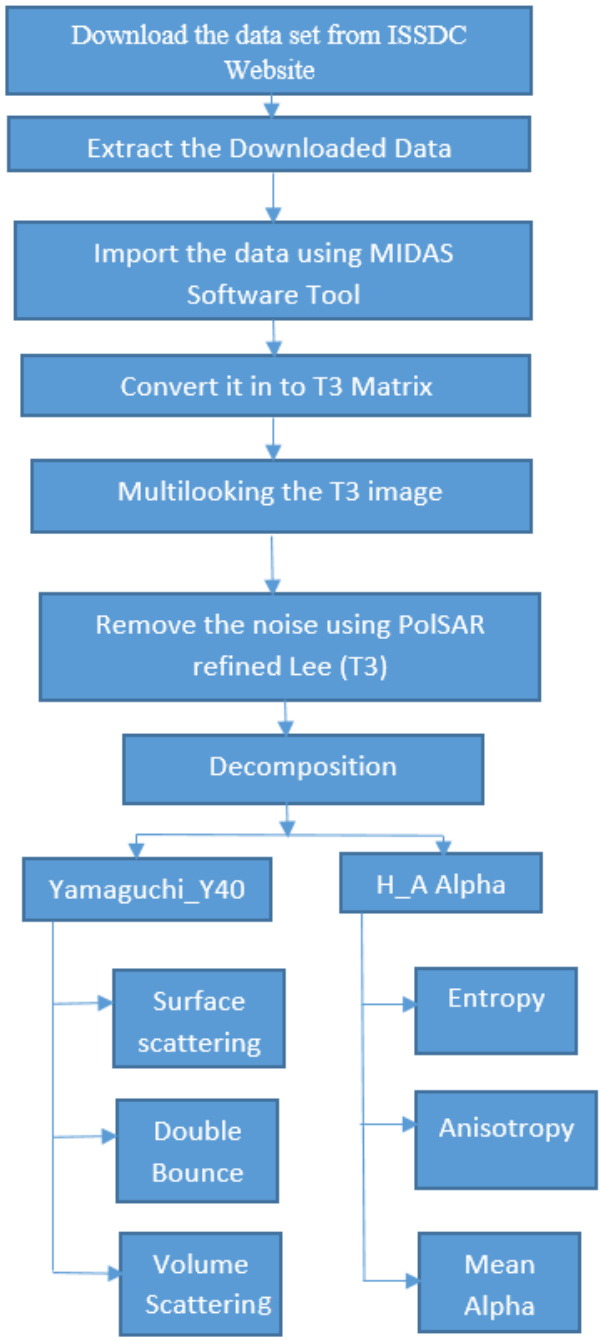

Fig. 2. Methodological flow chart for the polarimetric processing of the L-band DFSAR data.

for generation of 2x2 complex matrix from this matrix can extract the information of radar reflection. Polarization state and scattering information is available in fully polarimetric radar scattering theory.

A. Radiometric Processing

To understand the dual polarization or full polarization of back scattering elements can be derived using the radiometric backscattering coefficient (σ^0)

B. Covariance/Coherence Matrices

Covariance and coherency matrices are generated from backscattering elements. Based on radar reflection. In fully polarimetric mode , the DFSAR Transmits pulse to pulse in two orthogonal polarizations and receive the reflected signal in orthogonal polarizations in the similar base used in transmission , based on these reflections complex scattering matrix is generated, it is related to the electric field of two dimensional transmitted and received signals. The scattering matrix [S] describes how a radar signal interacts with a target while capturing of both transmission and reception signals and polarization states of the radar signal. However, system distortions can be calculated from difference between scattering matrix [S_measured] and actual scattering matrix [S_actual]. scattering matrix can be expressed as

$$\begin{bmatrix} S_{HH} & S_{HV} \\ S_{VH} & S_{VV} \end{bmatrix}_{\text{measured}} = K(\gamma)[R] \begin{bmatrix} S_{HH} & S_{HV} \\ S_{VH} & S_{VV} \end{bmatrix}_{\text{actual}} [T] \tag{1}$$

$$[R] = \begin{bmatrix} f_r(\gamma) & \delta_1^r(\gamma) \\ \delta_2^r(\gamma) & 1 \end{bmatrix} \tag{2}$$

$$[T] = \begin{bmatrix} f_t(r) & \delta_1^t(\gamma) \\ \delta_2^t(\gamma) & 1 \end{bmatrix} \tag{3}$$

C. Multilooking

The polarimetric data processing was done using MIDAS [3].Each scattered image has been multilooked using the following formula:

$$\text{Multilook Factor} = \frac{\text{Line Spacing}}{\text{Pixel Spacing} \times \sin(\theta)} \tag{4}$$

Around 300 datasets acquired up to season 3 are processed to generate the mosaics [7].

D. Filtering

After generation of covariance/coherence matrices and multilooking need to preserve the edges, MIDAS tool provides different polarimetric and amplitude filters [8]. Refined lee filter [5x5] performs the filtering the data sufficiently in homogeneous regions and reduces the speckle noise of the DFSAR data.

E. Polarimetric Decomposition

Scattering decompositions are widely utilized in polarimetric radar data analysis to enhance interpretation, extract physical data, facilitate segmentation, and function as a preliminary step for the inversion of geophysical parameters.. To understand the distribution of water ice deposits, the scattering mechanism from the radar data can be helpful.Hermit-A crater is located at North Polar Region the maximum area is PSR, this region is experienced with minimum sunlight, it creates a cold conditions it may lead to preservation of water ice. The Hermite-A crater is a promising site for analyzing the potential availability of water on the surface of the moon. This data can be derived from the second-order scattering matrices, like the [T] or [C] matrices, which are generally divided into two primary categories: decompositions based on eigenvectors and eigenvalues, and decompositions based on models citeb9. MIDAS provides extensive capabilities for performing different polarimetric decompositions on both fully polarimetric and hybrid-polarimetric data.

The scattering mechanism of fully polarimetric decomposition modeling is utilized to extract information through various scattering mechanisms. The Yamaguchi decomposition technique, also referred to as a four-component decomposition model, provides an analysis of scattering in four categories: even bounce, odd bounce, surface, and helix scattering. It is important to note that this Yamaguchi decomposition algorithm does not fulfill the requirement for reflection symmetry. The effectiveness of this decomposition model relies on essential coherency matrices derived from surface, double-bounce, volume, and helix scattering components. The total power of this model is the aggregate of all individual scattering components.

$$\langle [T] \rangle = f_s \langle [T] \rangle_{\text{surface}} + f_d \langle [T] \rangle_{\text{double}} + f_v \langle [T] \rangle_{\text{volume}} + f_c \langle [T] \rangle_{\text{helix}} \tag{5}$$

Where, $\langle [T] \rangle$ denotes the coherency matrix, $\langle [T] \rangle_{\text{surface}}$ denotes surface scattering, $\langle [T] \rangle_{\text{double}}$ denotes double bounce scattering, $\langle [T] \rangle_{\text{volume}}$ denotes volume scattering, and $\langle [T] \rangle_{\text{helix}}$ denotes helix scattering. Additionally, f_s is the surface scattering contribution, f_d is the double bounce scattering contribution, f_v is the volume scattering contribution, and f_c is the helix scattering contribution.

IV. RESULTS AND DISCUSSION

Hermite-A crater located at North Pole, maximum part of the crater located in PSR region and it is bowl- shaped structure so it is referred to as a twin of Shackleton. The diameter of this crater is around 20km, the coordinates of Hermit-A crater is $87.8°$N and $47.1°$oW. The Fig.3(a) is the seleno referenced image from this image coherency 3x3 matrix[T] is generated as illustrated in Fig.3(b). Based on the polarization theory, backscattering values are represented in the form of coherency matrix, from this values we understood the characteristics of the lunar surface. Following this, multi-look processing was applied to the [T] matrices to evaluate the scattering mechanisms of distributed targets. The multilooking process also created square pixels by averaging the matrices [9]. This step helps in reducing speckle noise using a refined Lee filter with a 5x5 window as shown in Fig.3(c), though it also slightly reduces the azimuth resolution [10]. Since SAR images are produced by coherent processing of returns from consecutive pulses, there is pixel-to-pixel intensity variation, which appears as a granular effect known as speckle [11]. One common method to mitigate speckle is by averaging several independent reflectivity estimates.After generating the [T3] matrix applying multilooking, and reducing speckle, the three regions on the inner crater's wall, rim, floor, and ejecta are more clearly identifiable, as shown in Fig.3(d).

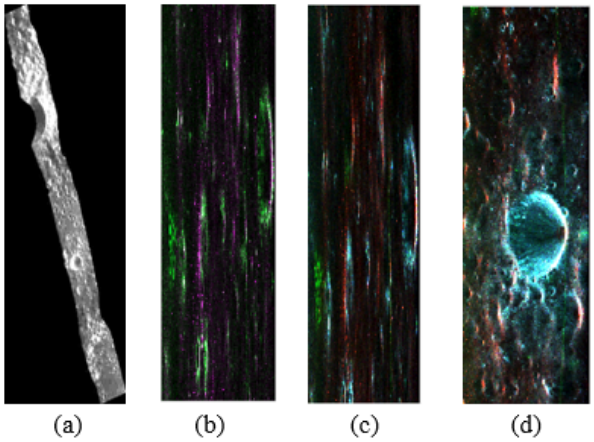

Fig. 3. (a) SRI Image (b) T3 Matrix_Image (c) PolSAR Refined Lee (T3) (d) Mutlilook

A. H(Entropy)-A(Anisotropy)-alpha decomposition:

This method utilizes the three eigenvalues of the coherence matrix[T3] to find outs the three principal polarimetric parameters: entropy (H), anisotropy (A), and mean alpha angle $\bar{\alpha}$. Entropy (H) represents the degree of randomness in the scattered and the depolarization of the microwave signal. Low entropy values ($H < 0.3$) indicate coherent, highly polarized scatterers, whereas high entropy values are associated with distributed targets [8]. Anisotropy calculate the relative significance of the second and third eigenvalues, especially useful when $H > 0.7$. Mean alpha angle $\bar{\alpha}$ defines the nature of the scatterer and the kind of scattering mechanism. Values of $\bar{\alpha} \leq 40°$ indicate surface scattering, while $40° < \bar{\alpha} \leq 60°$ suggests volume scattering, and $\bar{\alpha}$ values between $60° - 90°$ correspond to double-bounce scattering [12]. Representation of RGB in H-A-Alpha decomposition red color signifies the double bounce scattering, green color denotes the volume scattering and blue color indicates the surface scattering as shown in Fig.4.

B. Yamaguchi Decomposition

Yamaguchi decomposition plays important role to know the characteristics of lunar surface, it generates three com-

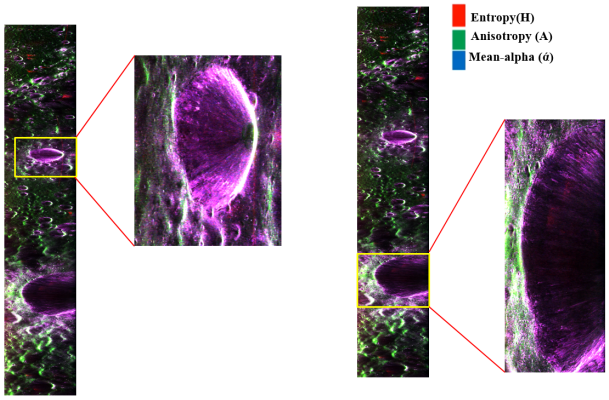

Fig. 4. H-A-alpha Decomposition of chandrayaan-2 (DFSAR)

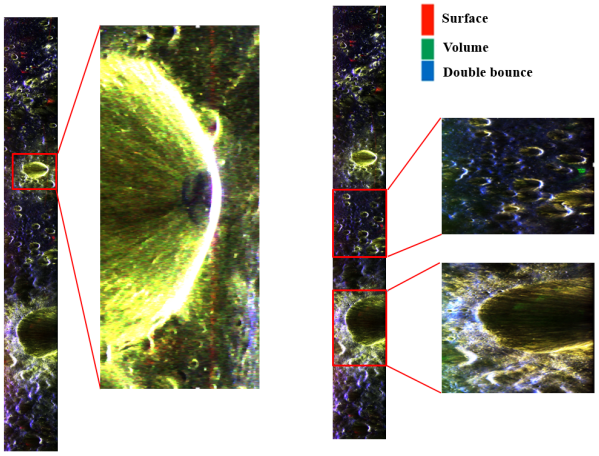

Fig. 5. Yamaguchi Decomposition of chandrayaan-2 (DFSAR)

ponents odd, even and volume bounce scattering as shown in Fig. 5. This decomposition can be achieved using MIDAS software it provides the provision of Y40, Y4R and G4U under yamaguchi decomposition method. It introduces the helix component for SAR observation at nonsymmetrical cases [13]. Yamaguchi-4R has angle adjustment to its ancestor Y40 and hence, the scattering behavior can be represented with RGB, here red indicates odd bounce scattering, green color indicates the volume scattering and blue represents the even bounce scattering [14]. Fresh craters are very rough at wavelength- scales, fresh excavated rocks, impact melt, and rough terrain. High CPR Value inside and outside crater rim erosion does not distinguish between inside and outside [15]. Anomalous and fresh craters have high CPR inside rim, low CPR outside likely to be caused by presence of water ice (i:e stable in permanent darkness). The visual outputs produced by MIDAS clearly demonstrated distinctions among different lunar surface features and offered valuable insights into their physical properties. In summary, the results highlight the efficacy of utilizing calibrated L-band DFSAR data alongside advanced processing tools like MIDAS for thorough polarimetric analysis, providing significant revelations about the lunar surface and its attributes.

V. CONCLUSION

In conclusion, the study employed both H-A-Alpha and Yamaguchi decomposition techniques to characterize the L-band DFSAR data from Chandrayaan-2 for better polarimetric analysis compare with[3-5] at specifically targeting the Hermite-A crater. The H-A-Alpha decomposition successfully identified the scattering processes within the crater region, highlighting the prevalence of volume scattering in the walls and floor, along with some surface and double-bounce scattering observed in the more even areas. This provided detailed insight into the roughness and structural properties of the crater's surface. Meanwhile, Yamaguchi decomposition, particularly the Y4R variant, offered enhanced characterization of scattering mechanisms by incorporating the helix scattering component, which is not addressed in simpler models. This allows better differentiation between odd, even, volume, and helix scattering, improving the accuracy of surface interpretation. The integration of these decompositions minimizes overestimation of particular scattering types and enhances understanding of the surface and structural properties of lunar craters. Together, these methods present a comprehensive approach to analyzing polarimetric SAR data, offering nuanced insights into surface scattering phenomena.

With the recent availability of fully polarimetric synthetic aperture radar (SAR) data of the lunar surface from the DFSAR, a noteworthy avenue for further research has emerged. This involves investigating potential fundamental differences in the capabilities of various radar architectures, such as Fully Polarization (FP) versus Circular Polarization (CP), in measuring the polarimetric properties of the lunar surface. We intend to carry out a series of comparative studies utilizing monostatic radar data by acquiring new DFSAR data sets with comparable viewing angles in the near term. In particular, our goal is to compare (i) DFSAR FP and CP data gathered at the same wavelength, and (ii) DFSAR S-band FP and CP data against the Mini-RF S-band data.

ACKNOWLEDGEMENT

The authors would like to thank ISRO-HQ (Indian Space Research Organization-Head Quarters) for financial Support. The authors would like to thank the Manipal Academy of Higher Education for funding the registration fee and travel expenses.The authors also extend their thanks to the ISSDC Pradan website for providing DFSAR data sets and MIDAS tool.

REFERENCES

[1] Bhiravarasu SS, Chakraborty T, Putrevu D, Pandey DK, Das AK, Ramanujam VM, Mehra R, Parasher P, Agrawal KM, Gupta S, Seth GS. Chandrayaan-2 dual-frequency synthetic aperture radar (DFSAR): Performance characterization and initial results. The Planetary Science Journal. 2021 Jul 23;2(4):134.

[2] K. Dasari and A. Lokam, "Exploring the Capability of Compact Polarimetry (Hybrid Pol) C Band RISAT-1 Data for Land Cover Classification," in IEEE Access, vol. 6, pp. 57981-57993, 2018, doi: 10.1109/ACCESS.2018.2873348.

[3] Maganti ST, Chakraborty T, Chirakkal S, Putrevu D, MIsra A. A Software Tool to Process and Analyse Chandrayaan-2 Polarimetric Dual-Frequency SAR (DFSAR) Data. In53rd Lunar and Planetary Science Conference 2022 Mar (Vol. 2678, p. 2232).

[4] Putrevu D, Chakraborty T, Bhiravarasu SS, Das A, Pandey DK, Mukhopadhyay J, Misra A. POLARIMETRIC BEHAVIOUR OF VARIOUS LUNAR IMPACT CRATERS DERIVED FROM CHANDRAYAAN-2 DUAL-FREQUENCY SAR FULL-POL L-BAND ACQUISITIONS. In53rd Lunar and Planetary Science Conference 2022 Mar (Vol. 2678, p. 1916).

[5] Putrevu D, Das A, Vachhani JG, Trivedi S, Misra T. Chandrayaan-2 dual-frequency SAR: Further investigation into lunar water and regolith. Advances in Space Research. 2016 Jan 15;57(2):627-46.

[6] Mazarico E, Neumann GA, Smith DE, Zuber MT, Torrence MH. Illumination conditions of the lunar polar regions using LOLA topography. Icarus. 2011 Feb 1;211(2):1066-81.

[7] R. K. Raney, "Comparing Compact and Quadrature Polarimetric SAR Performance," in IEEE Geoscience and Remote Sensing Letters, vol. 13, no. 6, pp. 861-864, June 2016, doi: 10.1109/LGRS.2016.2550863.

[8] Dasari K, Anjaneyulu L. Importance of Speckle filter window Size and its impact on Speckle reduction in SAR images. International Journal of Advances in Microwave Technology (IJAMT). 2017;2(2):98-102.

[9] Kiran D, Anjaneyulu L. Eigen Value and Eigen Vector Based Decomposition and Wishart Supervised Classification on Fully Polarimetric SAR Data. Indian Journal of Science and Technology. 2016 Dec;9(S1):1-6.

[10] Maganti T, Chakraborty T, Putrevu D, Bhiravarasu SS, Das A, Pandey DK, Ramanujam VM, Mehra R, Gupta S. First Ever Circular Polarization Ratio (CPR) and Radar Scattering Map of Lunar Poles in L-Band Using Full-Pol Chandrayaan-2 DFSAR Data. LPI Contributions. 2023 Mar;2806:1993.

[11] Hajnsek , Irena, Eric Pottier, and Shane R. Cloude. "Inversion of surface parameters from polarimetric SAR." IEEE Transactions on Geoscience and Remote Sensing 41.4 (2003): 727-744.

[12] N. Bhogapurapu, A. Bhattacharya and Y. S. Rao, "Chandrayaan-2 Dual Frequency Synthetic Aperture Radar (DFSAR) Full and Compact Polarimetric Data Analysis for the Lunar Surface," 2021 7th Asia-Pacific Conference on Synthetic Aperture Radar (APSAR), Bali, Indonesia, 2021, pp. 1-5, doi: 10.1109/APSAR52370.2021.9688528.

[13] U. Shroff, S. Shukla, P. Patel and S. Mohan, "Detection of Water Ice in Faustini Crater Floor Using DFSAR," IGARSS 2024 - 2024 IEEE International Geoscience and Remote Sensing Symposium, Athens, Greece, 2024, pp. 6096-6099, doi: 10.1109/IGARSS53475.2024.10641024.

[14] S. Kumar, V. Chaudhary, A. Singh and P. Chauhan, "Scattering-based Analysis of South Polar Crater of the Lunar Surface Using L-band SAR Data of Chandrayaan-2 Mission," 2021 IEEE International India Geoscience and Remote Sensing Symposium (InGARSS), Ahmedabad, India, 2021, pp. 459-462, doi: 10.1109/InGARSS51564.2021.9791981.

[15] X. Zhao, Y. Deng, H. Han, H. Zhang, X. Liu and D. Liu, "Investigating the Residual Polarimetric Distortion and Removing the Low-Quality Area of Chandrayaan-2 Dual-Frequency Synthetic Aperture Radar Full-Polarization Images," in IEEE Transactions on Geoscience and Remote Sensing, vol. 62, pp. 1-17, 2024, Art no. 5208317, doi: 10.1109/TGRS.2024.3378449.